



Stellenbosch

UNIVERSITY
IYUNIVESITHI
UNIVERSITEIT

Mechatronics Skripsie Report: Tip-thrust Rotary-wing Aircraft

Mechatronic Project 478
Final Report

Author: Rayde Krüger
24723061

Supervisor: Dr. A Gill

2024-11-11

Department of Mechanical and Mechatronic Engineering
Stellenbosch University
Private Bag X1, Matieland 7602, South Africa.

Plagiarism declaration

I have read and understand the Stellenbosch University Policy on Plagiarism and the definitions of plagiarism and self-plagiarism contained in the Policy [Plagiarism: The use of the ideas or material of others without acknowledgement, or the re-use of one's own previously evaluated or published material without acknowledgement or indication thereof (self-plagiarism or text-recycling)].

I also understand that direct translations are plagiarism, unless accompanied by an appropriate acknowledgement of the source. I also know that verbatim copy that has not been explicitly indicated as such, is plagiarism.

I know that plagiarism is a punishable offence and may be referred to the University's Central Disciplinary Committee (CDC) who has the authority to expel me for such an offence.

I know that plagiarism is harmful for the academic environment and that it has a negative impact on any profession.

Accordingly all quotations and contributions from any source whatsoever (including the internet) have been cited fully (acknowledged); further, all verbatim copies have been expressly indicated as such (e.g. through quotation marks) and the sources are cited fully.

I declare that, except where a source has been cited, the work contained in this assignment is my own work and that I have not previously (in its entirety or in part) submitted it for grading in this module/assignment or another module/assignment. I declare that have not allowed, and will not allow, anyone to use my work (in paper, graphics, electronic, verbal or any other format) with the intention of passing it off as his/her own work.

I know that a mark of zero may be awarded to assignments with plagiarism and also that no opportunity be given to submit an improved assignment.

Signature:

Name: Rayde Andrew Krüger Student no: 24723061

Date: 25/10/24

Guidelines for the use of AI in M&M

Skripsie

16 September 2024

When using AI in their M&M final year projects, students must:

1. Add an AI Use Declaration (see last page of this document) to the front matter of the final report
2. Add a section to Chapter 1 of their report (typically the last section in Chapter 1) that declares the use of all AI tools (if any) and clearly states where and how it was used.

1 Overview

This document is composed of modified extracts from the “Draft interim SU guidelines on allowable AI use and academic integrity in assessment” and from a similar document used in the Mechatronics 424 module.

The purpose of this document is to provide concise requirements to students on the responsible use of generative Artificial Intelligence (AI) and Large Language Models (LLM) in the final year project (skripsie) that are in line with current institutional policy. The policy, and therefore the guidelines in this document, are subject to change.

2 Responsible use of AI

The key principles when using AI for students translate to being accountable for what you produce through critically engaging with AI-generated output. This means being transparent, accurately attributing ideas and ensuring that the work is still authentic and not an uncritical submission of AI output as your own.

2.1 Accountability

You are responsible for what you create and how it impacts others and society. AI tools don't have accountability. It is thus your responsibility to ensure that work submitted under your name is factually correct and not likely to cause harm, i.e., through spreading false information, misappropriation or sharing of personal information.

2.2 Authenticity

It is your responsibility to ensure that you know the requirements (i.e., whether AI use is allowed) for each assessment task. The default assumption should be that it is not allowed. When allowed, you need to guard against outsourcing your learning to AI. You may potentially use AI tools to assist where relevant and where permitted by the module, but not to complete the assessment on your behalf.

When using AI, critically engage with AI-generated output, ensuring that any output you retain accurately presents your position and voice. Consider how you will make a case for the work being authentically yours, i.e., can you answer detailed questions or explain why you chose a certain direction, referred to a certain author, drew a specific conclusion e.g., in an oral or interview? Do you understand the content, and can you explain it in your own words? Can you summarize key ideas from the content?

2.3 Transparency

You should clearly and honestly declare the use of AI tools and their outputs as well as the extent of the use, i.e., refer to the ‘search strategy’ and rationale that informed this. Consider questions such as: why was this the most appropriate approach or option, what are the limitations, etc.?

Review the privacy settings of your AI application account/s with the provider/s to ensure you are aware of what data is being collected and how it is being used (in the Terms and Conditions when registering).

2.4 Fairness

Your use of AI tools/systems should be ethical and responsible and should comply with academic integrity standards. Be cautious of misusing AI-generated output since this output could be false and could also result in misrepresenting your own abilities. You should always be able to provide evidence of your understanding and the process/methodology you followed to reaching an answer. **The use of AI may limit your preparedness for subsequent assessments.**

3 AI use in M&M Final Year Project

Table 1 has been modified from the source document, to indicate the acceptable use of AI for the M&M final year project module.

M&M SKRIPSIE - USE OF AI

Table 1: AI use in M&M Final Year Project

AI use for	This use is similar to	Requirements for use in final year project
Ideation phase		
Brainstorming ideas eg topic or approach	Discussing the idea with a friend or tutor	You must keep a record of the prompts you used and the outputs you received
Creating an outline or a plan	Google search or checking Wikipedia	It is your responsibility to critically engage with the output of the AI tool and check the accuracy of the output
Drafting phase		
Learning about a particular topic	Google search or checking Wikipedia	You need to (1) find the original owner of the idea and (2) ensure that all content is factually correct and not likely to harm anyone through spreading untruths or sharing personal information
Searching for literature on a topic	SU library and database or a Google Scholar search	Always check that references are real, suitably academic and include the key works. Include URLs of all references. Also check for similarity; some research tools offer near direct quotes without indicating it as such
Generating or drafting a coherent output, ie using AI to complete the assessment (or part thereof) on your behalf	Enlisting someone else to write your paper or complete your project for you	This is not allowed. Submitting content generated via AI or using paraphrasing or translation software tools on texts you did not personally write or make a substantial input to, and did not reference, will be deemed as academic misconduct
Revising phase		
Language editing	Similar to using a spelling checker	Language enhancement tools are increasingly available in word processing software (such as MS Word) and tools such as Grammarly are also increasingly popular. Always save a draft of your original text as backup and remember to check the accuracy of the suggestions made by language editing software. Make sure that the authenticity of your text is not compromised
Soliciting feedback	Asking a friend or tutor to read your work and offer you feedback	You may be asked to provide evidence of your learning process, ie copy of the feedback and how you responded to it. Remember that you are ultimately accountable for your work and that you should feel comfortable with the improvements you incorporate
Revising a piece of work	Asking someone else to improve the content of your work	This is not allowed. Submitting work revised by AI undermines the learning outcomes and will be deemed as academic misconduct

AI Use Declaration

1. I am convinced and can support my claim that my assessment product is an indication of my own learning, knowledge, skills, and understanding.
2. Where I have used AI tools for enhancing my own creation of ideas and words, I acknowledge that I have to declare it.
3. Where I have used AI tools for generating new ideas, words, code, image-prompts for other AI Image-generating tools, or structure and even presentations (or other AI tools that can be used as assistants to the knowledge building and representing process), I have declared and documented the use of such tools and I am prepared to talk about the process I used and what it contributed to my learning and insights.
4. I am aware that the lecturer can ask me to demonstrate my learning, for example through explaining the choices I made in terms of approach, content used, literature selected, conclusions drawn, etc. through an additional assessment like an oral (for example).
5. I understand that if I am not able to agree to the above points, there is a chance that my academic behavior will be deemed unethical and might lead to a disciplinary case being brought against me on the grounds of cheating or plagiarism and that the standard procedures for such behavior will be followed.
6. As per the Disciplinary Code of SU (par. 10.2.1 and 10.2.2) I understand that I take responsibility for the integrity of my work, which includes the obligation to ask for clarification from an academic member of staff if I am unsure of anything, and that I strictly adhered to all instructions received in the course of the academic assessment by relevant and authorized staff (whether the instruction is in oral or written format).
7. I understand that when I am not able to document and declare my use of AI tools, this behavior will be deemed as cheating in examinations and assessments (Disciplinary Code 1.1 c.) as I referred to “unauthorized notes, books, electronic devices or other reference material”.

Student Number	Signature
Initials and Surname	Date

Executive summary

Title of Project
Tip-thrust rotary aircraft
Objectives
The main objective is to design, build and test a prototype of a tip-thrust rotary aircraft with controllable pitch to create directional thrust.
What is current practice, and what are its limitations?
Current tip-thrust rotary aircraft either use traditional methods for pitch control, such as a swashplate, or use a fixed pitch rotor with additional methods for propulsion to control direction.
What is new in this project?
This project investigates the use of a variation of tip-thrust to control the pitch of the rotor.
If the project is successful, how will it make a difference?
The controlling pitch using a variation of thrust will decrease the mechanical complexity of rotary aircraft, removing failure points as well as making them easier to produce, lighter and cheaper.
What are the risks to the project being a success? Why is it expected to be successful?
There is a risk that the pitch cannot change by a large enough amount or fast enough to allow for directional thrust. This risk is reduced through the correct selection and sizing of the components.
What contributions have/will other students made/make?
Previous student have studied drones, including the thrust produced by the rotors, which will assist in choosing a propulsion method.
Which aspects of the project will carry on after completion and why?
The control system and optimization of the design can be made to the proof of concept using the mathematical model.
What arrangements have been/will be made to expedite continuation?
By documenting the procedure, steps followed, including what each component does and how they interact with each other as well as a project folder will assist any future further contribution.

Acknowledgements

I would like to say thank you to Dr. A. Gill for assisting me to develop this concept to propose as well as for his guidance throughout the project. The insight and encouragement provided was invaluable to this project. I would also like to thank the laboratory engineers and technicians especially as Mr. K. Neaves and Mr. F. Zietsman for their assistance while designing and for manufacturing the components of the proof of concept.

Table of contents

List of symbols	xiv
1 Introduction	1
1.1 Background	1
2 Modelling the System on MATLAB	2
2.1 Modelling the Rotor	2
2.2 Modelling the Propellers	4
2.3 Optimization of Tip Thrust Positions	6
2.4 Combined Model	7
2.5 Pitch Model	7
2.5.1 Step Input	8
2.5.2 Sinusoidal Input	9
3 Design	11
3.1 Rotor	11
3.2 Rotor Hub	12
3.2.1 Electronics	13
3.3 Final Design	14
4 Software	15
4.1 System Interaction	15
4.2 Position and Speed Detection	16
4.3 Control System	17
5 Experimentation	18
5.1 Aim	18
5.2 Equipment	18
5.3 Procedure	19
5.3.1 Test Descriptions	19
6 Data Analysis, Results and Discussion	21
6.1 Sensor Validation and PID Performance	21
6.2 Data Processing	23
6.3 Results and Discussion	25

6.3.1	Comparison to Mathematical Model	25
6.3.2	Directional Flight	26
7	Future Development and Conclusion	28
7.1	Future Development	28
7.2	Conclusion	28
8	List of references	30
A	Microcontroller Circuit	31
A.1	Pin Out Table	31
A.2	Full Circut Diagram	32
B	Mechanical Drawings and Design	33

List of tables

6.1	PID values	22
A.1	Pin out table	31

List of figures

2.1	Thrust predicted over the length of the rotor	3
2.2	Torque predicted over the length of the rotor	3
2.3	Rotor thrust vs angular velocity	4
2.4	Rotor torque vs angular velocity	4
2.5	Propeller thrust versus speed graph	5
2.6	Propeller torque versus speed graph	5
2.7	Coefficient P1	6
2.8	Coefficient P2	6
2.9	Coefficient P3	6
2.10	Thrust available and required for tip-thrust positions	7
2.11	Optimization curve	7
2.12	Pitch change sinusoidally	8
2.13	Free body diagram of tip thrust	8
2.14	System response to a step input	8
2.15	System response to a sinusoidal input	9
2.16	Torque surface graph	10
3.1	NACA profiles	11
3.2	Sectioned view one rotor	12
3.3	Sectioned hub view	12
3.4	Circuit block diagram	13
3.5	Annotated final design	14
4.1	Main function code flow chart	15
4.2	Timing diagram for forward flight	16
4.3	PID controller diagram for 1 rotor	17
5.1	Testing setup	19
6.1	Pitch from sensor vs. actual pitch	22
6.2	Angular velocity from sensor vs. actual angular velocity	22
6.3	Pitch sweep	22
6.4	FFT at 60 rpm	23
6.5	Natural frequency of the system	23
6.6	Unfiltered load cell data	24
6.7	Filtered load cell data	24

6.8 Predicted vs. actual lift produced	25
6.9 A section of the pitch response for forward flight mode	26
6.10 Forward directional lift	26
6.11 Reverse directional lift	26
6.12 Input vs. output thrust	27
A.1 Circuit Diagram	32

List of symbols

Constants

$$\rho = \text{air density } 1.225 \text{ kg/m}^3$$

Variables

C_L	Coefficient of lift	[]
C_{L_0}	Lift coefficient offset	[]
C_{L_α}	Lift coefficient gradient	[]
C_D	Coefficient of drag	[]
V_0	Axial component of air flow velocity	[m/s]
V_0	Axial component of air flow velocity at disk	[m/s]
V_1	Resultant flow velocity	[m/s]
V_2	Radial component of air flow velocity	[m/s]
V_∞	Free-stream velocity	[m/s]
V_ω	Far wake velocity	[m/s]
α	Angle of attack	[Deg]
θ	Pitch	[rad]
ϕ	Angle made from thrust and lift	[Deg]
R	Blade length	[m]
c	Blade chord	[m]
T	Thrust	[N]
Q	Torque	[N·m]
L	Drag	[N]
b	Tip loss coefficient	[]
C_T	Thrust coefficient	[]
B	Number of blades	[]
ω	Angular velocity	[rads/s]
A	Area	[m ²]
ζ	Damping ratio	[]

<i>I</i>	Current	[A]
----------	-------------------	-----

Subscripts

<i>rotor</i>	Rotor
<i>Prop</i>	Propeller
<i>motor</i>	Tip-thrust/TORB brushless motors
<i>n</i>	Natural frequency

Abbreviations

AOA	Angle of Attack
ESC	Electronic Speed Controller
FFT	Fast Fourier transform
PWM	Pulse Width Modulation
TORB	Thrust On Rotor Blade
VTOL	Vertical Take-off and Landing

Chapter 1

Introduction

1.1 Background

Helicopters are said to be the only aircraft that, since their conception, has saved more lives than they have taken (Anderson and Eberhardt (2010)). Their high level of mobility, vertical take off and landings and their ability to hover give helicopters great versatility. Helicopters are the most common example of a rotary wing aircraft and are used in environments ranging from rocky mountains to stormy seas. With such high stakes it is vital to minimize points of potential failure. Two of these failure points in a helicopter are the tail rotor and the swashplate. The tail rotor is required to counter the torque produced by the engine which turns the main rotor to produce thrust. If the tail rotor were to stop working, the helicopter would lose its controllability and would have to land immediately. A tip thrust rotary aircraft places the propulsion on the tips of the aircraft's rotor and thus does not produce any torque that needs to be canceled, eliminating the need of a tail rotor. By using the tip thrust propulsion on a rotor rather than a conventional drone, better hovering efficiencies can be obtained. Using tip thrust could potentially eliminate the need for mechanical complexity of traditional rotary aircraft. One of these mechanisms being the swashplate of a helicopter, which controls the pitch and is responsible for creating directional thrust. Similarly to the tail rotor, this is a critical component and requires constant maintenance to ensure the complex mechanism does not fail.

This paper will research, design, construct and test a tip thrust rotary aircraft which will actuate the pitch of the rotor through the use of propulsion situated on each blade. Traditionally, swashplates change the rotor's pitch for portions of its rotation, this creates an unbalanced distribution of lift force, causing the aircraft to move in the desired direction.

The aim is to develop a rotary-wing aircraft in which rotor pitch is controlled by the tip thrust. The primary objective is to produce directional thrust by using the tip thrust to imitate the cyclic action created by a traditional swashplate.

Chapter 2

Modelling the System on MATLAB

To aid in creating the first design, a mathematical model is required to determine the metrics of the system. This allows for rapid testing and optimization of parameters.

2.1 Modelling the Rotor

To model the rotor, Blade Element Theory analysis was applied as described by Aerodynamics for Students (2024). The rotor was divided into segments and the lift and drag for each segment were calculated. This gives the profile of the thrust and torque along the rotor as can be seen in Figure 2.1 and Figure 2.2, respectively. The sum of each segment will result in the total thrust and torque produced by the rotor. The thrust and torque produced by each segment is an iterative process as the incoming flow velocity is unknown. In the first iteration, it is assumed to be zero, and thus the angle of attack is equal to the pitch of the rotor. The incoming air can be calculated using the first approximation of thrust and with Newton's First Law:

$$F = ma$$
$$T = \frac{d(mV)}{dt}$$

Assuming air above the rotor is stationary

$$T = \dot{m}V$$
$$T = \rho V_{disk} A V$$

This gives the thrust in terms of the air velocity and velocity at the disk. As stated by momentum theory and by Gessow and Garry C. Myers (1985), the far wake velocity is half that of the air velocity V at the disk. Thus, for hover,

assuming the free stream velocity is zero, the axial velocity at the disk can be given by

$$T = (\rho\pi R^2 V_{disk})2V_{disk}$$

$$V_{disk} = \sqrt{\frac{T}{2\rho\pi R^2}}$$

Using this and the angular rotation of the rotor, the angle of attack can be found as

$$\alpha = \theta - \arctan\left(\frac{V_{disk}}{\frac{2}{3}R\omega_{Rotor}}\right)$$

Two-thirds of the blade's length is used as the speed of the blade is not constant along its radius, so the speed of the centroid was used to try to approximate the average angle of attack along the blade. It was seen that the thrust and torque converge after 25 iterations. Resulting in the profiles as seen in Figure 2.1 and Figure 2.2.

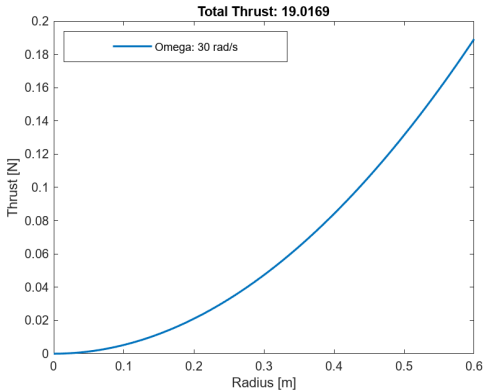


Figure 2.1: Thrust predicted over the length of the rotor

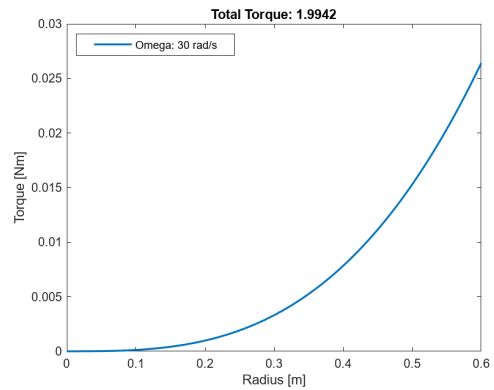


Figure 2.2: Torque predicted over the length of the rotor

Using 300 segments resulted in predictions that are 0.5% different from the value obtained using five thousand segments. This was an acceptable value and was used to reduce the computational cost of the model.

The Blade Element analysis considers the 2D segments and thus does not take 3D effects into account. This results in the model underpredicting the torque and overpredicting the thrust produced. One of the assumptions neglects the tip vortices which will decrease the thrust produced. To compensate for the decreased thrust, the predicted thrust can be multiplied by a tip-loss factor b . Gessow and Garry C. Myers (1985) describe the tip-loss factor as a coefficient that is multiplied by the radius of the rotor for the thrust calculations. This assumes that from $b \times R$ of the rotor, it will produce zero lift but still have

drag. It is defined as

$$b = 1 - \frac{\sqrt{2C_T}}{B} \quad (2.1)$$

where B is the number of blades

C_T is the rotor thrust coefficient

The thrust coefficient is the thrust per unit blade span and can be defined as

$$C_T = \frac{T}{\pi R^2 \rho (\omega_{Rotor} R)^2} \quad (2.2)$$

The above gives the lift profile along each blade of the rotor, but finding the total thrust for different angular velocities is more vital for designing the initial proof of concept. To do this the thrust and torque values were calculated for a range of angular velocities and their values were stored. An exponential function is then fitted onto these equations, as can be seen in Figure 2.3 and Figure 2.4, resulting in two equations that can be used to predict the amount of thrust and torque produced for a given angular velocity, Eq. 2.3 and Eq. 2.4, respectively.

$$T = 0.01805\omega_{Rotor}^2 \quad (2.3)$$

$$Q = 0.002216\omega_{Rotor}^2 \quad (2.4)$$

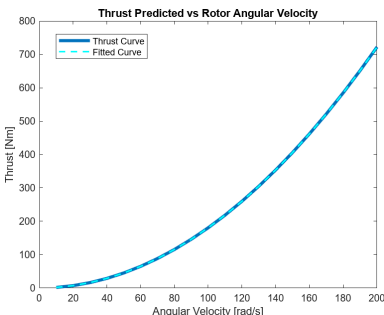


Figure 2.3: Thrust predicted vs angular velocities and the fitted exponential equation

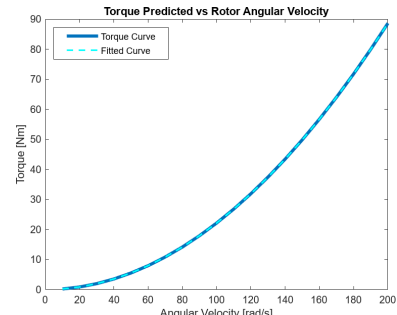


Figure 2.4: Torque predicted vs angular velocities and the fitted exponential equation

2.2 Modelling the Propellers

Modeling the propellers for the tip thrust used a similar approach as for the rotor except that the propellers are smaller, and the accuracy is not as crucial for designing the proof of concept. The thrust and torque produced were calculated using one section with the radius being two-thirds of the blade

length as this was shown to give an accurate value with one section when compared to multiple sections.

The propeller's pitch is described by the distance the propeller moves forward per rotation and thus to find the average angle of the pitch it can be found as

$$\theta_{prop} = \arctan\left(\frac{\text{Pitch}}{\pi d}\right)$$

The incoming airflow of each propeller can be found by multiplying the angular velocity of the rotor by the position along the rotor blade of the propellers. The high velocities of the inflowing air will decrease the angle of attack. This requires the propellers to have high angular velocities to ensure an angle of attack that produces thrust. Choosing a propeller with a high pitch can ensure that the incoming air meets the blade at a more effective angle of attack.

As the incoming air velocity is dependent on the angular velocity, this results in a thrust and torque versus the angular velocity of the propellers to have a different shape depending on the angular velocity. This can be seen in Figure 2.5 and Figure 2.6.

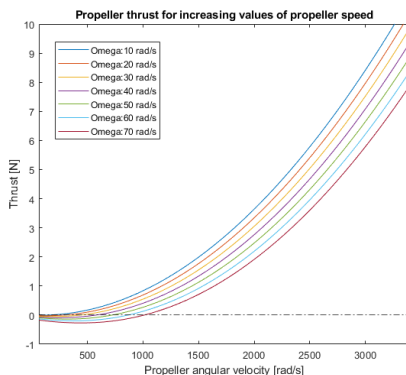


Figure 2.5: Propeller thrust versus its speed for different values of rotor angular velocity

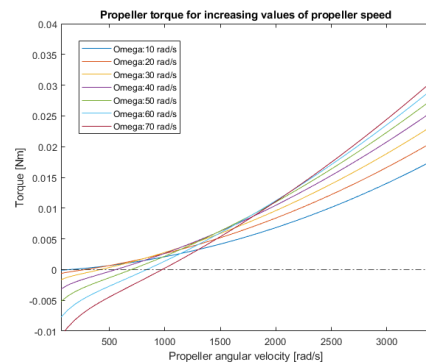


Figure 2.6: Propeller torque versus its speed for different values of rotor angular velocity

Each graph for the thrust, however, can be fitted by a parabolic graph, but with different coefficients depending on the rotor's angular velocity. The solution for this was to find a relationship between the coefficients and the rotor's angular velocity. The change of these coefficients can be seen in Figure 2.7, 2.8 and 2.9, in which

$$T_{prop} = P_1 \omega_{prop}^2 + P_2 \omega_{prop} + P_3$$

From these graphs, clear relationships can be seen with all three coefficients and the angular velocity. Fitting curves to each coefficient result in the Eq. 2.5,

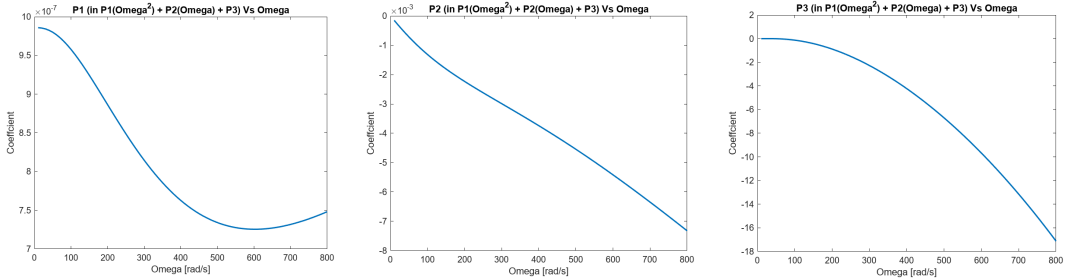


Figure 2.7: Coefficient P1 Figure 2.8: Coefficient P2 Figure 2.9: Coefficient P3

which fully describes the thrust produced by tip-thrust.

$$\begin{aligned}
 T_{prop} = & ((-2.500 \times 10^{-16})\omega_{rotor}^3 + (1.517 \times 10^{-12})\omega_{rotor}^2 + (-1.314 \times 10^{-9})\omega_{rotor} \\
 & +(1.037 \times 10^{-6})\omega_{prop}^2 + ((-7.806 \times 10^{-12})\omega_{rotor}^2 + (7.144 \times 10^{-9})\omega_{rotor}^2 \\
 & +(-1.301 \times 10^{-5})\omega_{rotor} - 0.0003)\omega_{prop} + ((-4.593 \times 10^{-5})\omega_{rotor}^2 \\
 & +(-1.006 \times 10^{-3})\omega_{rotor} + 0.2227)
 \end{aligned} \tag{2.5}$$

2.3 Optimization of Tip Thrust Positions

As previously mentioned the incoming airflow for the tip thrust is equal to the position of the tip thrust multiplied by the rotor's angular velocity. Having the propulsion at the end of the rotor will maximize the torque produced, however, it will have a higher incoming airflow and require higher rotation from the tip-thrust motors to produce thrust.

The optimum point of the tip-thrust motors would be where the thrust required for the torque is minimized, and the thrust produced is maximized. To find the optimum point the rotor angular velocity and tip thrust angular velocity were kept constant at an expected operating value. The thrust produced by the motors as well as the thrust that would be required to produce the torque were calculated for each percentage length along the rotor as seen in Figure 2.10. This took the hub diameter into account, thus at 0% of the rotor span (i.e. the base of the rotor), the torque does not tend to infinity.

The thrust required and thrust available were standardized, so they could be compared. The two standardized sets of values were subtracted from each other and the turning point of the resulting graph was used as the optimized position along the rotor. As can be seen in Figure 2.11, this is around 32.5% along the rotor blade. While this does vary slightly depending on the motor's angular velocity, at the expected velocity a position of 32.5% of the rotor is optimum and is close to the mean for the position that incorporates the range of motor speed.

As the thrusts will no longer be placed on the tip of the rotors, it was believed that they should be referred to as TORB motors (Thrust On Rotor Blade)

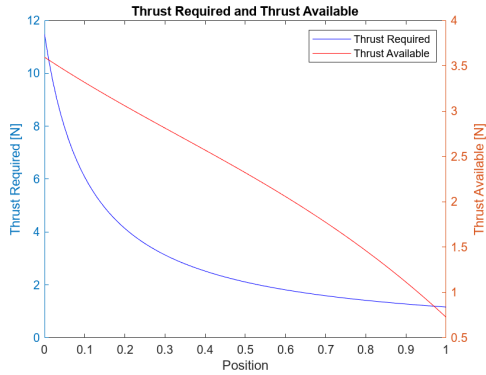


Figure 2.10: Thrust available and the thrust required for a position along the rotor

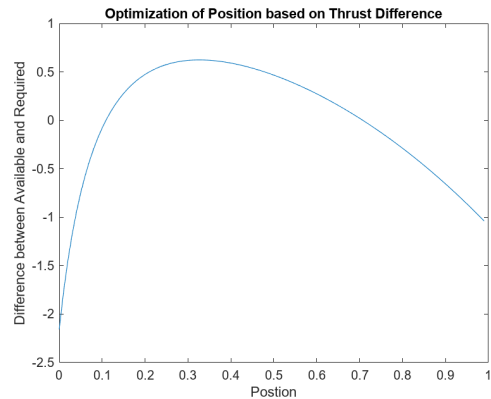


Figure 2.11: Optimization curve

from this point forward. This was chosen to give a more accurate name to this method of creating rotational actuation.

2.4 Combined Model

Using the models created above, the system can take the amount of thrust required and will output the torque produced and required thrust.

$$\omega_{rotor} = \sqrt{55.4T_{rotor}} \quad (2.6)$$

$$Q_{Rotor} = 0.1228T_{rotor} \quad (2.7)$$

2.5 Pitch Model

To estimate the amount of torque required to change the pitch of the rotor a rotational mass-spring-damper model was created. This models the system which assumes there will be natural damping, so no artificial damping will be introduced, and the system will be rotating on a low friction bushing, thus the effects of friction have been neglected. The model assumes a value for the moment of inertia based on a CAD model of the rotor.

Two models have been created, one for a step input to achieve a fixed pitch change and a second one to achieve a varying pitch to create sinusoidal output which can be seen in Figure 2.12. This will create a differential amount of thrust that will induce forward movement. For these two models, the control of the steady state of the system was the objective, and thus the rise time and overshoot was a lower priority.

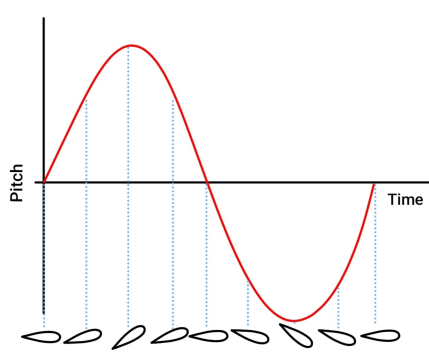


Figure 2.12: Pitch change sinusoidally

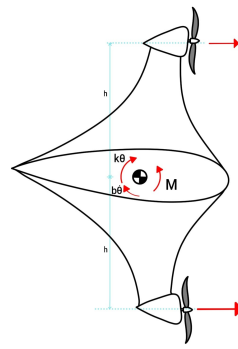


Figure 2.13: Free body diagram of tip thrust

2.5.1 Step Input

From Figure 2.13, a differential equation can be derived for a step input to give Eq. 2.8.

$$\ddot{\theta} + 2\omega_n \zeta \dot{\theta} + \omega_n^2 \theta = \frac{M_{\text{required}}}{I_{\text{airfoil}}} \quad (2.8)$$

As no artificial damping will be added to the system, it was assumed to be an under-damped system and an arbitrary dampening coefficient has been used, and it is assumed it is starting where θ and $\dot{\theta}$ is zero. Using this information, the solution to Eq. 2.8 given by Eq. 2.9.

$$\theta(t) = Ae^{-\zeta\omega_n t} \sin(\omega_d t + \phi) + \frac{M_{\text{required}}}{k} \quad (2.9)$$

$$\text{where } A = \frac{-\frac{M_{\text{required}}}{k}}{\sin(\phi)}$$

$$M_{\text{required}} = \theta_{\text{required}} k$$

θ_{required} is the desired pitch

Figure 2.14 shows the system response to an applied moment that results in

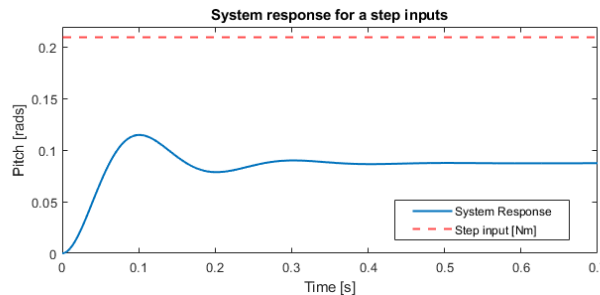


Figure 2.14: System response to a step input

a steady state of 0.0873 rads (5°). It can be seen that the response from the system has some oscillation, however its settling time is reasonably fast and would suffice for the proof of concept.

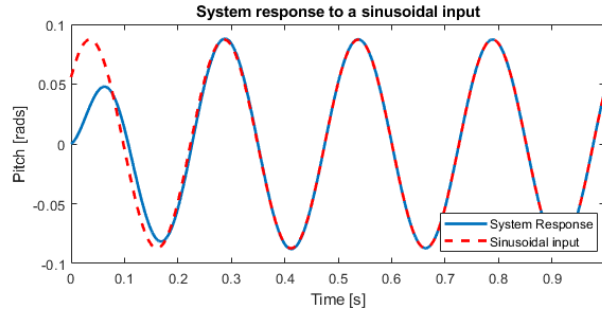


Figure 2.15: System response to a sinusoidal input

2.5.2 Sinusoidal Input

For a sinusoidal input the differential equation is given by Eq. 2.10

$$\ddot{\theta} + 2\omega_n\zeta\dot{\theta} + \omega_n^2\theta = \frac{M_{\text{required}}}{I_{\text{airfoil}}} \cos(\omega_{\text{rotor}}t) \quad (2.10)$$

The same dampening coefficient which was used for the step input was used for the sinusoidal input. This differential equation can be solved by Eq. 2.11

$$\omega(t) = Ae^{-\zeta\omega_n t} \sin(\omega_d t + \phi) + X \cos(\omega_{\text{rotor}} - \beta) \quad (2.11)$$

To find the torque required for a given steady state, first X must be determined. It can be seen that the exponential term will tend to zero as time tends to infinity, thus $X = \theta_{\text{required}}$. Knowing this, the moment can be given by

$$M_{\text{required}} = XI_{\text{airfoil}} \sqrt{(\omega_n^2 - \omega_{\text{rotor}}^2)^2 + (2\zeta\omega_n\omega_{\text{rotor}})^2}$$

This produces the graph as seen in Figure 2.15. To find the optimum spring stiffness and damping coefficient which will produce the smallest required torque, these two parameters were changed, and the torque required was plotted vs these parameters resulting in the graph as shown in Figure 2.16. With reference to the damping coefficient, it shows that the lower the coefficient, the lower the torque, however, this will affect how much the system's natural frequency influences the output. For the spring constant, it should be noted that there is a value for which the torque is minimized. After further inspection, it can be seen that choosing a spring constant which results in the natural frequency being close to ω_{rotor} will require the lowest amount of torque to control.

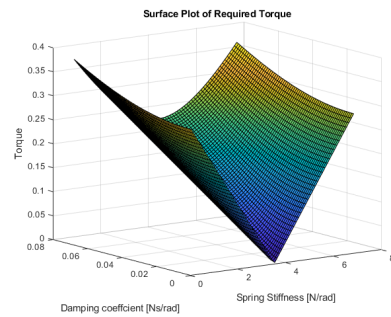


Figure 2.16: Surface graph showing of torque versus damping coefficient and spring stiffness

Chapter 3

Design

Using the values obtained from the mathematical models, the rotary aircraft can be designed. The two main components to design are the rotors and the hub. These need to have an interface together as well as with the microcontroller and other electronics.

3.1 Rotor

A NACA 4415, shown in Figure 3.1 was used for the rotors as it has a good a high coefficient and a low drag coefficient, which allows the rotor to produce Large amount of thrust at low angular velocities. Using the points to create



Figure 3.1: NACA profiles

the NACA 4415, the shell of the rotor was extruded. A rib system was created inside the rotors to minimize the weight while maximizing the strength of the rotors. The length and width was determined to be 600 mm and 150 mm, respectively. The rotor's center of pressure is around 25% along the chord of the rotor, by placing a shaft through this point would ensure that these forces do not create a moment on the rotor.

As mentioned before the thrust will be positioned 32.5% along the rotor blade. This reduces the incoming air speed that the tip-thrust propellers experience, however, it will require more thrust to produce the required torque.



Figure 3.2: Sectioned view one rotor

3.2 Rotor Hub

The second subsystem is the hub of the rotary wing aircraft. The purpose of the hub was to interface with the rotors, contain its components and to connect the spinning rotor with the stationary main body.

For the hub the electronics and microcontroller will all be spinning with the rotor and send data to another transceiver module connected to a second microcontroller. Each of the hub level, shown in Figure 3.3, is used to house different components and each of these levels, besides the interface hub, can be interchanged. The hub needs to be connected to the nonrotating body.

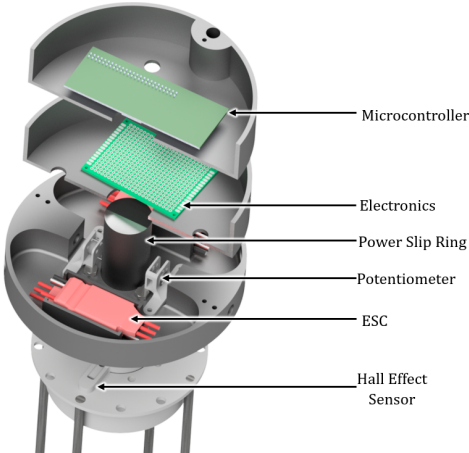


Figure 3.3: Concept 2 rotor hub

This is done with a hollow shaft. The shaft needs to enclose the power slip-ring. It is flange mounted to the hub, using the same bolts used to fix the slip ring into place. The shaft's diameter then decreases to act as a shoulder that locates the top thrust bearing. This top bearing supports the weight of the

hub and rotor before the thrust produced equals the weight of the rotor-hub assembly. The shaft at the end is threaded to allow a lock nut to be tightened onto it. This lock nut is used to locate the bottom bearing, which will support the thrust produced by the rotor and transmit it to the main body. Since the data that is being transmitted will be done wirelessly, it may be subject to interference, however it won't be noisy. The issue with using the wireless module is that it has a maximum transfer rate of 2 Mbs, this is fast enough for what is required, but it does set a limit for future values. While it can become battery powered, it currently can be connected straight to a power supply, this allows uninterrupted testing. While it currently has a slip-ring, it can be removed in later iterations, which can reduce the overall torque required to accelerate the rotors to their desired speed.

3.2.1 Electronics

To detect speed and position, Hall effect sensors have been used. By using two, the angular velocity of the rotor and the position can be determined. One Hall effect sensor has been placed to detect a magnet once every revolution, this is used to calculate the angular velocity. The second hall effect sensor detects eight magnets, each placed 45° from each other, allowing the position of the rotor to be known to the nearest 45° .

A potentiometer is used to determine the pitch of the rotor. This is done by connecting the potentiometer's dial to the shaft of the rotor, such that when the rotor pitches up or down, the resistance of the potentiometer increases or decreases. A voltage is applied to the potentiometers and by measuring the change in voltage across the potentiometer, the value can be associated with an angle to measure the pitch of the rotor.

These are all controlled by the microcontroller, the STM32 Discovery board

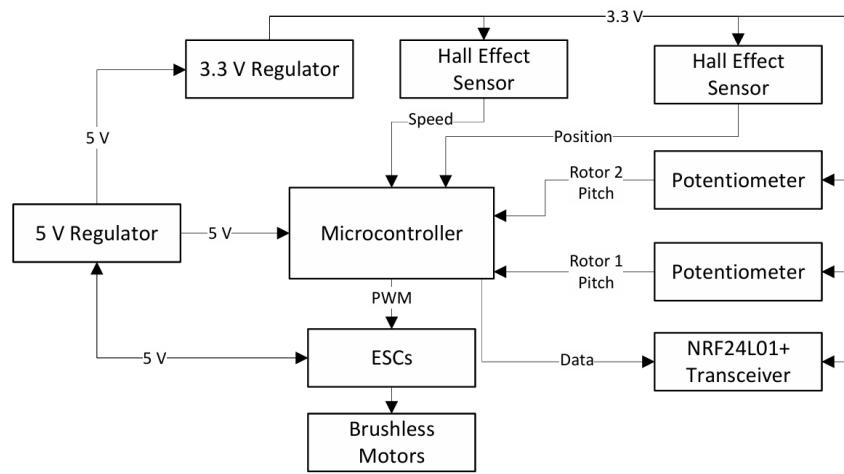


Figure 3.4: Circuit block diagram

as shown in Figure 3.4. It takes the input data from the Hall effect sensors and

the potentiometers and calculates what the required PWM signal should be for the brushless motors. All this data is then sent back to the computer using the NRF24l01+ transceiver module, using the library from Yaqoob (2018).

3.3 Final Design

The final design will use a power slip-ring to power the brushless motors and send data using a transceiver module. Figure 3.5 shows the proposed layout for the final design.

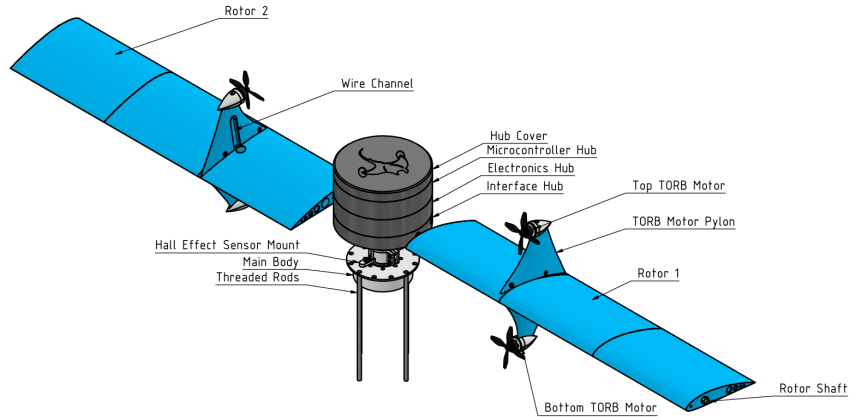


Figure 3.5: Annotated final design

The rotor has the rotor shaft running through it and a nut is used to secure the segments in place between the main body and the last segment. A spring is connected to the hub and to the rotor to help support the rotor and maintain its default position. The shaft then goes through the hub and is held in place with a circlip. The shaft then connects to the potentiometer to measure the pitch. The main body then connects to the support shaft which is held in place between two thrust bearings with a lock nut to allow the hub to spin while the body remains stationary. Inside the support shaft is the slip ring and its wires to provide power to the whole device.

Chapter 4

Software

4.1 System Interaction

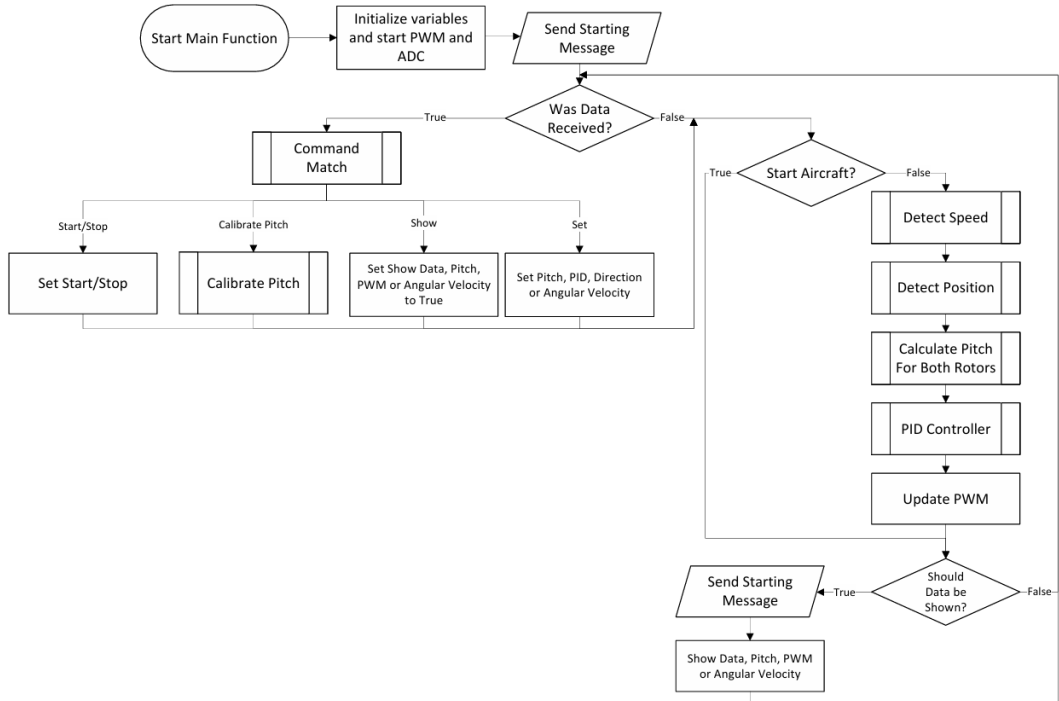


Figure 4.1: Main function code flow chart

Figure 4.1 shows a high level overview of the main function which shows how the subsystems integrate into the main system. During start up of the main loop, it initializes the interrupts, PWM and analog to digital converter (ADC). The program then enters the main loop where it checks if data has been received and whether the system must start. If the system has been started, it reads the inputs and uses these inputs to determine the speed of the motors to obtain the required pitch and angular velocity. The input and output values are then sent back, and the loop repeats itself. Before the system should

be started, the system should be calibrated to ensure the potentiometers are accurately measuring the pitch. The ADC of the microcontroller was used to measure the potentiometer's voltage, and converted into pitch using two equations, from -45° to 0° and 0° to 45° to increase the accuracy.

4.2 Position and Speed Detection

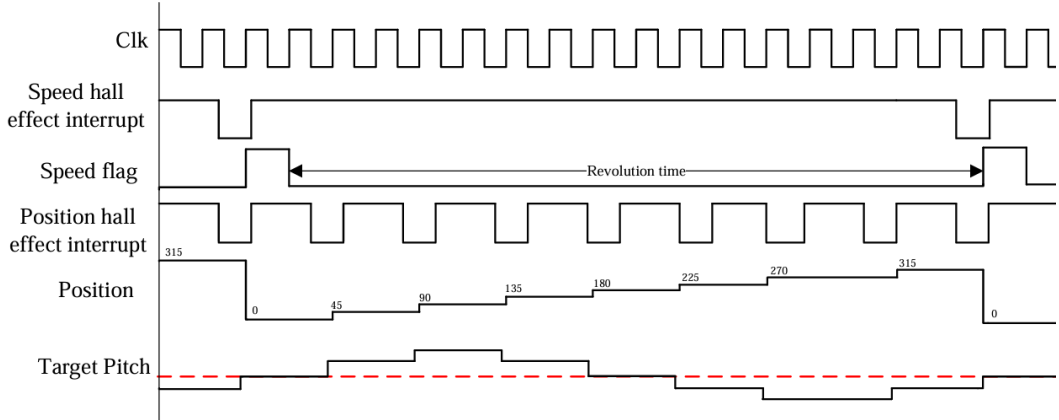


Figure 4.2: Timing diagram for forward flight

To determine the speed and position of the rotor two Hall effect Sensors were used. This Hall effect Sensor is connected to a microcontroller pin which has been configured as an external interrupt which is triggered on a falling edge. When the microcontroller detects the Hall effect's output signal go from high to low, it interrupts the code to set a flag. This indicates to the microcontroller to run the code to determine the angular velocity in the next iteration of code. The speed is determined by measuring the time in between these impulses, shown in Figure 4.2 as 'Revolution time', which is measured in milliseconds.

$$\omega_{rotor} = \frac{1}{\text{Revolution time}} \cdot 1000 \cdot 60 \quad [\text{rpm}]$$

Similarly, when the position hall effect's signal goes from high to low, a flag gets set. This causes the 'position' variable to be incremented by 45° , as each magnet is placed 45° from each other. This variable will continue to increment until the speed flag is set, which resets the position variable to zero, as illustrated in Figure 4.2. The position variable is used to adjust the target pitch of the to obtain the sinusoidal pitch change that is required for directional flight.

$$\theta_{target} = \Delta\theta_{rotor} \cdot \sin(\text{position} + \text{Directional Offset}) + \theta_{\text{Set Pitch}}$$

where

- $-\Delta\theta_{rotor}$ is the desired maximum that the pitch should change
- $-\text{Directional Offset}$ is used to change where the maximum and minimum thrust is produced to induced different directional thrust
- $-\theta_{\text{Set Pitch}}$ is the default pitch which it oscillates around

The target pitch for each rotor will have an offset of 180° to obtain the desired affect.

4.3 Control System

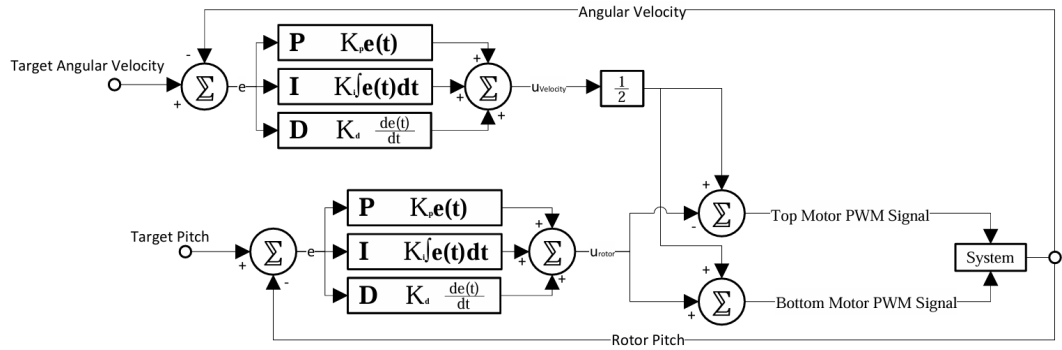


Figure 4.3: PID controller diagram for 1 rotor

Figure 4.3 shows the control system that is used to control the pitch and angular velocity for the aircraft. As illustrated, two PID controllers are used, one for angular velocity and one for the rotor pitch. Figure 4.3 shows the controller for one rotor. The first PID controller uses the current angular velocity and the target angular velocity to determine the PWM signal that needs to be maintained. This signal is then split between the two motors. To control the pitch, an additional PID controller is used, this determines by how much the top and bottom motors should be differed to obtain the moment to reach the required pitch.

Chapter 5

Experimentation

This chapter explains the experimental process created to measure overall lift, directional thrust produced and efficiency of the proof of concept created. It will explain the aim, equipment used and set-up.

5.1 Aim

The aim of these experiments is to validate the mathematical model, determine if directional thrust can be achieved with TORB control and to calculate the thrust efficiency of the aircraft.

5.2 Equipment

To measure the amount of lift created by the aircraft, the test bench, seen in Figure 5.1, was built using four 5 kg load cells. One load cell is placed at each corner to allow measurement of directional thrust. These load cells are each connected to a HX711 amplifier which is a 24-bit ADC which also amplifies the load cell's output and converts it to a digital reading. The data lines carry this reading to the STM32 Nucleo F411 microcontroller. This microcontroller is calibrated to convert the digital reading into weight. The microcontroller is also connected to the NRF24L01+ which receives the target speed, current speed, target pitch and current pitches from the aircraft.

The pitch and speed data is sampled at 100 Hz to prevent aliasing from occurring at higher rotational frequencies. Since the lift is expected to be a constant, a lower sampling rate is used to improve the accuracy of the readings. These readings are transmitted via UART to the computer's terminal. Figure 5.1 shows the full testing setup.

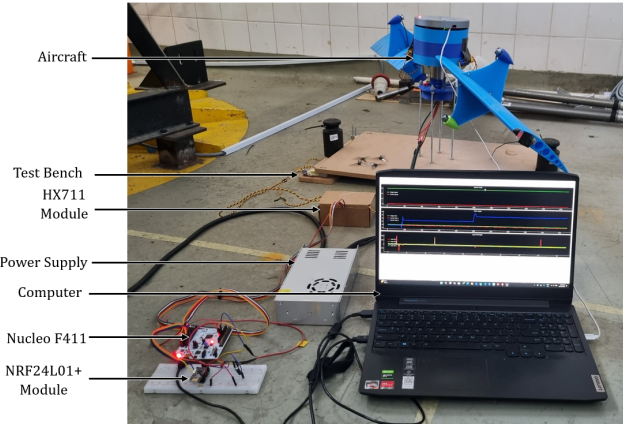


Figure 5.1: Testing setup

5.3 Procedure

5.3.1 Test Descriptions

Four different experiments will be performed to determine the response of the system. These are the locked rotor test, pitch, and speed sweep and directional flight test.

5.3.1.1 Locked Rotor Test

In this test, the rotor will be restrained so it cannot rotate. The purpose of this test is to determine the parameters of the PID control system. The Ziegler-Nichols tuning method (Franklin, Powell, Emami-Naeini, 2020) will be used to obtain an initial starting point for the PID and the parameters will be tuned during to the proceeding tests. During this test, a video of the rotor response will be captured to compare the results of the potentiometer's ability to determine the pitch compared to the actual pitch change.

5.3.1.2 Pitch Sweep

Once the PID has been tuned, its performance will be tested by setting the angular velocity and changing the pitch from 0° to 30° by increasing the pitch by 10° every 5 s. This will test the systems speed control system as well as the pitch control system while the system is operating.

5.3.1.3 Speed Sweep

Similar to the previous test, this test will be preformed by changing the target angular velocity from 40 rpm to 200 rpm. This will show the relationship between angular velocity and lift generated as well as the natural frequency of the system.

5.3.1.4 Directional Flight Test

This test will set the desired direction of the aircraft to determine whether the aircraft can create directional lift. It will test if the aircraft can create forward and reverse thrust.

Chapter 6

Data Analysis, Results and Discussion

6.1 Sensor Validation and PID Performance

The control system relies on the pitch which gets detected by each potentiometer and the speed and position detected by the hall effect sensors. These values were validated by comparing the results recorded by the sensor to the results measured after importing a video to Tracker (Douglas Brown, Wolfgang Christian, Robert M Hanson, 2024).

Figure 6.1 shows the pitch measured by the sensor versus the angle measured through Tracker. The results show that the potentiometer has a good estimate of the angle, however, it is not always reliable with smaller changes, potentially due to a loose interface. Although the potentiometer is not perfect, the accuracy gives an acceptable approximation for the proof of concept and, when calibrated correctly, proved to achieve satisfactory outputs. Figure 6.2 shows the angular velocity measured using the hall effect sensor versus the angular velocity measured using tracker. This shows that the sensor is closely matches to the actual speed, but it has a low resolution as it is updated once per revolution. This is acceptable as the angular velocity needs to reach and maintain a steady state and will not need a high resolution to achieve its function.

After validating the input data, the PID parameters could be tuned. To get the initial parameters, the Ziegler-Nichols method was used for the pitch. Using this the theoretical values for the PID were achieved. These values were further tuned until a satisfactory performance was obtained. The PID values for the speed was found through trial and error, giving the values in Table 6.1. The performance of the rotors PID response at 120 rpm can be seen in Figure 6.3. Rotor two manages to follow the trend of the target pitch, however has some steady state error. Rotor one is unstable and inconsistent. While it can follow the general trend, it is seen in the beginning that the system overshoots and oscillates when it has an error of 10° , however, later, in the same scenario, it remains constant. This could be due to the static resistance that is present in

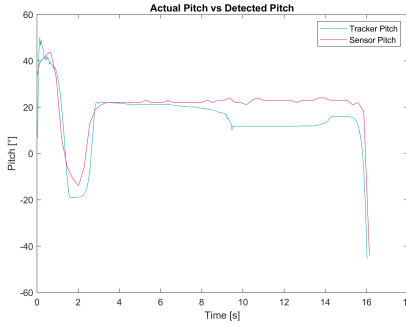


Figure 6.1: Pitch from sensor vs. actual pitch

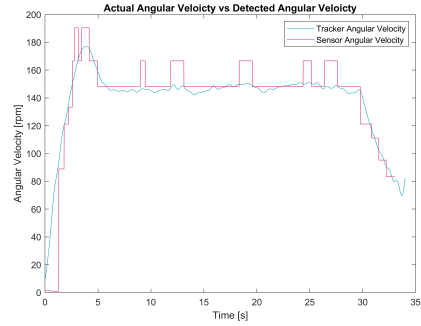


Figure 6.2: Angular velocity from sensor vs. actual angular velocity

Table 6.1: PID values

Control	P	I	D
Theoretical PID for Rotor 1	1.05	1.4	0.164
Actual PID for Rotor 1	1.05	1.5	0.2
Theoretical PID for Rotor 2	4.8	6.4	0.75
Actual PID for Rotor 2	4	5	1
PID for Angular Velocity	2	0.5	0.01

the potentiometer, which decreases as soon as this static friction gets overcome. Alternatively it could be due to the interaction of some aerodynamic forces as the control system was tuned using a static rotor, which does not have these forces. While the PID was tested and tuned during normal operation it was seen that the PID values that were ideal for one rotor speed, would be insufficient for another. The PID values which worked best across a range of angular velocities and flight modes was used, which are seen in Table 6.1.

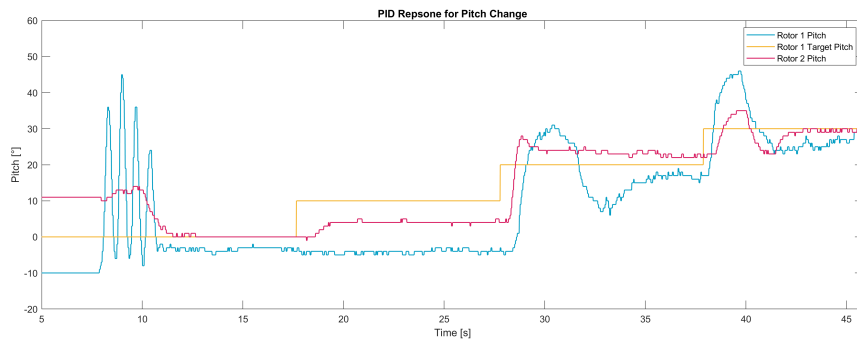


Figure 6.3: Pitch sweep

6.2 Data Processing

The data retrieved from the load cells need to be processed. Any outliers need to be removed as this would often be from an incorrect reading and the signal and gets converted from grams to Newtons. It was noticed that the readings had oscillations within them. A Fast Fourier Transform (FFT) was performed to determine the frequencies that these oscillations occur. As the sampling frequency for the load cell were 2.27 Hz, the Nyquist frequency would be 1.37 Hz. This implies that most of the rotor's rotational frequencies would experience aliasing and appear as a lower frequency. The resulting FFT can be seen in Figure 6.4, which shows a single sided FFT with frequencies present in the load cell data at 60 rpm. As shown the peak aligns with the aliasing frequencies that corresponds to the rotational frequencies. It can be implied that the rotational frequencies are responsible for these oscillations. A speed sweep was performed to determine the natural frequency of the system. Figure 6.5 shows that the only noticeable peak was around 0.01 Hz. This could relate to the rotational frequency of 135 rpm, or represents the lift produced. Further tests at a higher sampling frequencies would be needed to draw further conclusions.

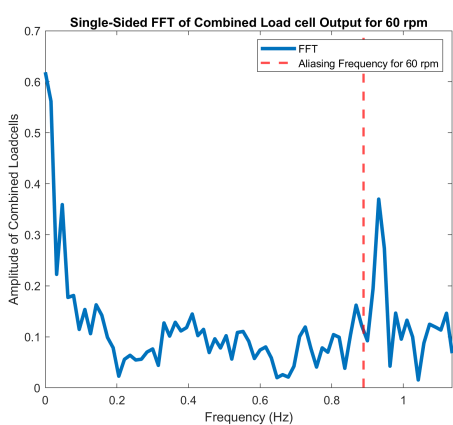


Figure 6.4: FFT at 60 rpm

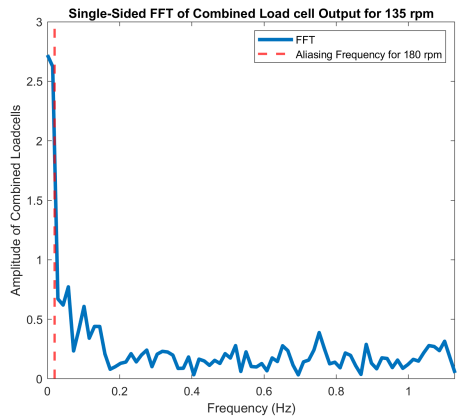


Figure 6.5: Natural frequency of the system

The decision to remove these higher frequencies was made. This was done with a Butterworth filter. This ensures that only the lift generated from the aircraft is shown without the interference of the physical system. The unfiltered and filtered data can be seen in Figure 6.6 and Figure 6.7, respectively.

Certain test required further data processing. Below illustrates the additional processing for certain tests

1. Mathematical Model Comparison

To Analyze the accuracy of the mathematical model, the thrust predicted

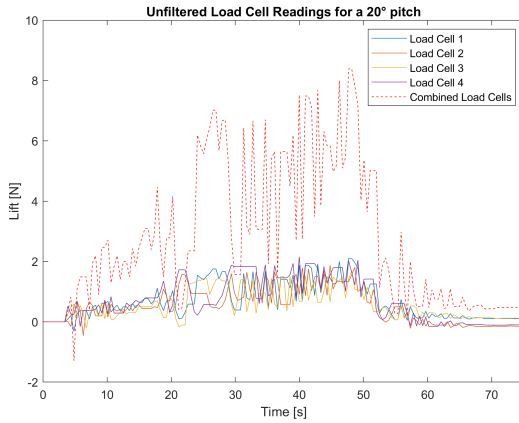


Figure 6.6: Unfiltered load cell data

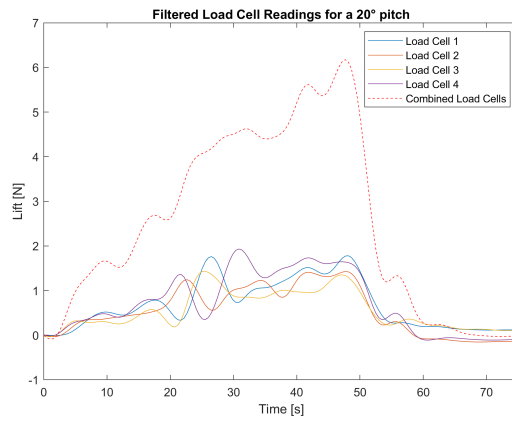


Figure 6.7: Filtered load cell data

by Eq. 2.3 was plotted using the measured angular velocity as the input to determine how closely the model matches the lift produced. The average rotor pitch was used as an indication of the overall pitch of the system and should be 20° to be comparable to Eq. 2.3.

2. Directional Thrust

The “front” of the aircraft is the midpoint between load cell 3 and 2. To determine whether directional thrust has been achieved, the difference between the thrust at the front and back will be examined.

$$\Delta T = (\text{Load Cell 1} + \text{Load Cell 4}) - (\text{Load Cell 2} + \text{Load Cell 3}) \quad (6.1)$$

This will produce a positive value for forward thrust and a negative value for reverse thrust. Due to gyroscopic precession, although the increased or decreased lift are at the midpoints of load cell 3 and 4 and load cell 1 and 2, this force will act at the midpoint of load cell 2 and 3 and at the midpoint of 1 and 4.

3. Efficiency

The PWM value of the TORB motors will be used to determine the thrust produced by the motors. This will be scaled according to the maximum thrust produced according to datasheet, which is 0.3 kg. The PWM value which corresponds with 0 thrust is 35 and maximum thrust is at 60.

$$T_{Prop} = \sum \frac{\text{PWM Signal}_{\text{motor}} - \text{Min PWM}}{\text{Max PWM} - \text{Min PWM}} \times \text{Max Thrust} \times 9.8 \quad (6.2)$$

This will estimate the amount of thrust produced by each TORB motor using the PWM signal. This, accompanied by the lift produced, the overall efficiency of the aircraft can be found as $\frac{\text{Output Thrust}}{\text{Input Thrust}}$.

6.3 Results and Discussion

6.3.1 Comparison to Mathematical Model

Figure 6.8 shows the relationship between the pitch, the angular velocity and the amount of lift produced. This also shows what the mathematical predicts the lift to be, this value and the actual lift has been scaled by 100. Initially, the model underpredicted the amount of thrust produced. To correct this, the thrust contributed by the TORB motors were added, resulting in the final formula to calculate the thrust produced for a pitch of 20° as shown in Eq. 6.3

$$T = \omega_{rotor}^2 \left(0.01805 + \frac{0.002216}{0.2625} \sin(20) \right) \quad (6.3)$$

After this correction has been added, Figure 6.8 shows that the model has a good estimate of the amount of lift produced until it reaches the higher angular velocities. Figure 6.6 shows that the oscillations become larger and more unstable at higher angular velocities. The issue could be solved by balancing the rotor to keep these oscillations to a minimum, or by increasing the rigidity of the base to prevent the oscillations becoming larger. Due to these larger oscillations, the testing was kept to lower angular velocities.

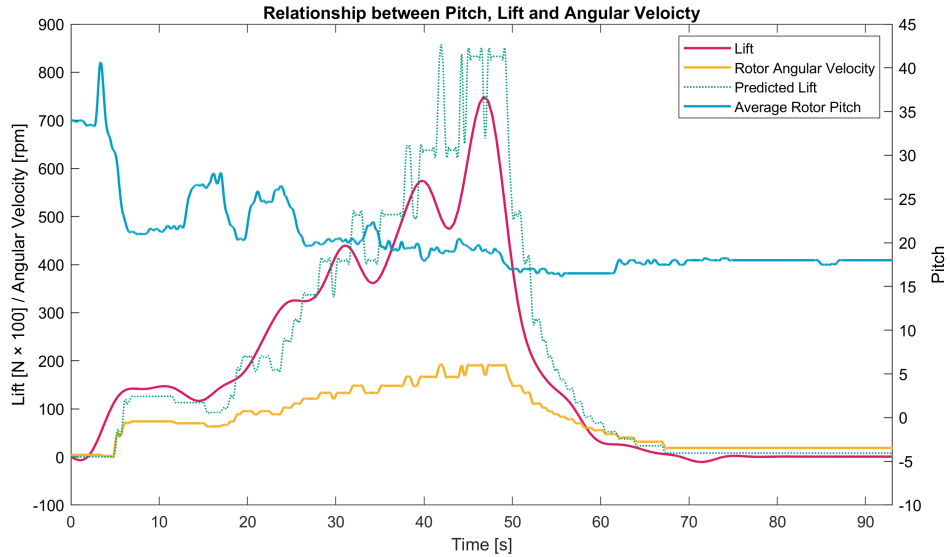


Figure 6.8: Predicted vs. actual lift produced

The average Root Mean Squared Error of all three test was 0.6529. This is 9.8% of the maximum thrust produced, which is an indication that the model is a good fit. Further investigation needs to be done to determine the cause for the deviation at higher angular velocities.

6.3.2 Directional Flight

Figure 6.9 shows the pitch for forward flight at 60 rpm. Rotor one is lagging slightly behind the control signal with rotor two being offset by 180° as it is physically 180° apart. While there is a large overshoot, the system performs how it is required to achieve directional thrust, mimicking the cyclic action of the swashplate. The graph for the reverse flight mode, not shown, shows the same large oscillations and slight lag, but again achieves the same effect of the cyclic action.

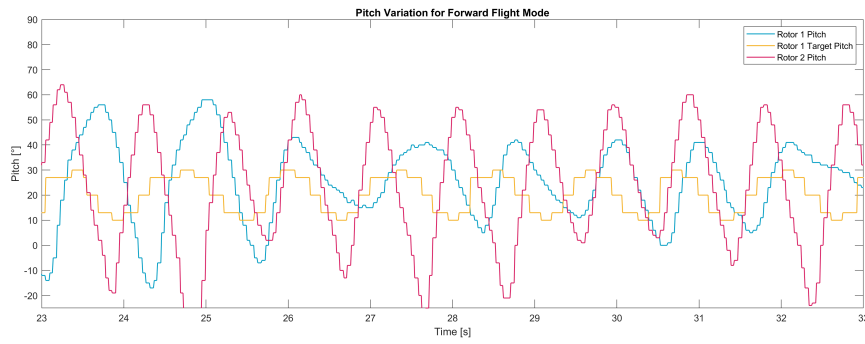


Figure 6.9: A section of the pitch response for forward flight mode

The resulting lift produced from the change in pitch observed in Figure 6.9 can be seen in Figure 6.10. As ΔThrust is positive this means that an upward force is being produced at load cell 1 and 4 while a downward force is being produced at load cell 2 and 3. This would tilt the aircraft forward, causing it to move forward. A similar phenomenon can be seen in Figure 6.11, except the flight mode has been set to reverse. These graphs show that at lower angular velocities, directional thrust can be achieved using just differential TORB.

Figure 6.12 shows the amount of lift that was generated by the aircraft com-

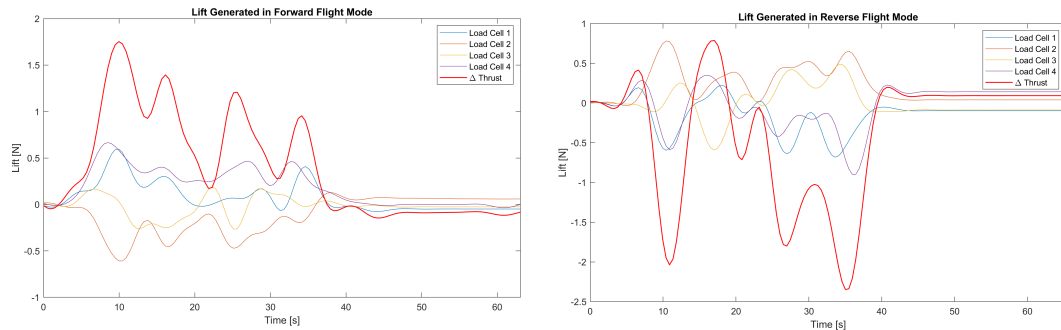


Figure 6.10: Forward directional lift

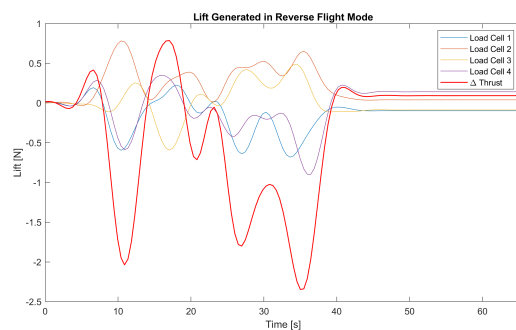


Figure 6.11: Reverse directional lift

pared to the total amount of thrust by the TORB motors. This resulted in an estimated thrust efficiency of 190% as the TORB motors is estimated to

generate an average of 2.2 N of total thrust and the aircraft produced an average of 4.2 N of thrust. As previously mentioned, some TORB thrust assists in generating lift. Accounting for this, the aircraft generates 3.45 N of thrust purely from the rotors. This greatly increases the aircraft's ability to hover, allowing it to remain in the air longer than conventional drones for the same power usage.

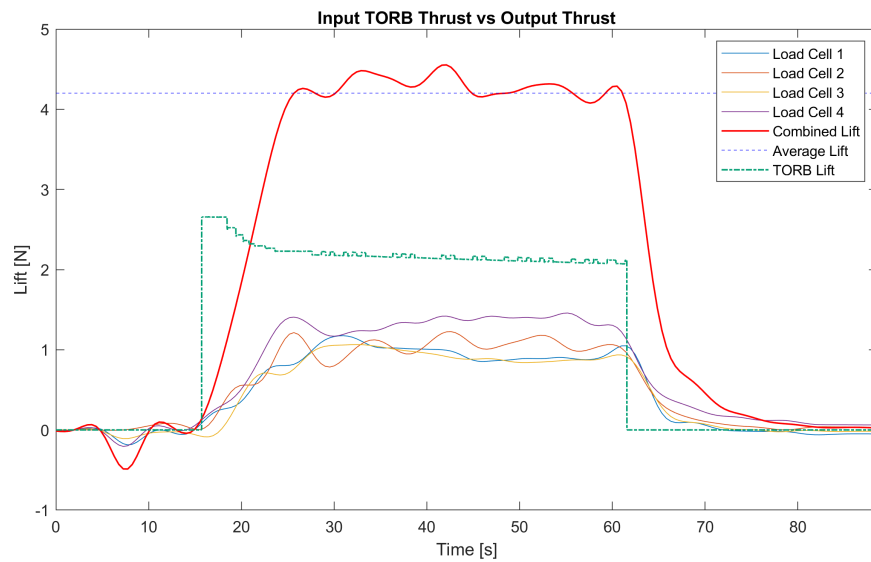


Figure 6.12: Input vs. output thrust

Chapter 7

Future Development and Conclusion

7.1 Future Development

The results obtained show the feasibility of the concept of using TORB to control the pitch of the rotors and warrants further development. The area which should be looked at is the control system and the elements surrounding it. Having a more accurate sensor to detect the pitch of the rotor would ensure that the correct pitch is being achieved by the control system. A more advanced control system would ensure a more stable and accurate control is achieved for higher angular velocities. Using the mathematical model, which has been validated, control systems such as lead/lag compensators or state space should be investigated.

Finally, if the system were to become airborne, the power source would need to be replaced with batteries. The aircraft would also need to have a stabilization system, which would require a gyroscope and its own control system.

7.2 Conclusion

The primary objective for this project was to design a tip-thrust rotary-wing aircraft which can control the pitch of the rotor using the tip-thrust. This was done to try to reduce failure points and reduce complexities these aircraft.

A MATLAB mathematical model of the system was created to adjust the physical parameters of the aircraft and to determine the speed of the rotor and thrust produced. This model also showed that placing the motors at the tip of the rotor would not be the most efficient, but should rather be placed 32.5% along the rotor. Using this knowledge, the rotor, thrust on rotor blades, hub and all the electronic components were designed.

The control of the aircraft was achieved using the STM32 Discovery board which uses PID controllers to determine the speed of the brushless motors. One of the PID controllers controlled the angular velocity while the others were focused on each rotor pitch. These controllers used potentiometers to get the error between the target and actual pitch and a hall effect sensor to determine the angular velocity of the aircraft to obtain the error.

The Potentiometers had a limited sensitivity for small adjustments, but overall had satisfactory performance. The hall effect sensor on the other hand was seen to be an accurate representation of the angular velocity of the system. Comparing the filtered data to the mathematical model showed that, the model had an average mean square error of 0.65, implying that the model fits the data well.

At lower angular velocities, the aircraft demonstrated its ability to create directional thrust controlled purely with the TORB motors. While testing, the PID control system revealed its instability, causing overshoots and oscillations. A more advanced control system should be looked into, which should increase the systems' stability. Despite this the aircraft demonstrated that it can imitate both collective and cyclic action of the swashplate while being 190% more efficient than using purely the TORB motors.

Going forward, a more advanced control system should be implemented to achieve the directional thrust at higher velocities. Using the mathematical model, which has now been validated, could be used to implement lead/lag control or state-space control.

Chapter 8

List of references

- Aerodynamics for Students (2024). Blade element theory for propellers. Accessed: 25 July 2024.
Available at: <https://www.aerodynamics4students.com/propulsion/blade-element-propeller-theory.php>
- Anderson, D.F. and Eberhardt, S. (2010). Helicopters and autogyros. In: *Understanding Flight*, 2nd edn, chap. 8. McGraw Hill, New York.
Available at: <https://www-accessengineeringlibrary-com.ez.sun.ac.za/content/book/9780071626965/chapter/chapter8>
- Douglas Brown, Wolfgang Christian, Robert M Hanson (2024). Tracker video and modeling tool.
Available at: <https://physlets.org/tracker/>
- Franklin, Powell, Emami-Naeini (2020). *Feedback Control of Dynamic Systems*. Pearson.
- Gessow, A. and Garry C. Myers, J. (1985). *Aerodynamics of the helicopter*. 8th edn. Fredrick Ungar Publishing Co., New York.
- Yaqoob, M. (2018). Tutorial 24 nrf24l01 radio transceiver.
Available at: <https://github.com/MYaqoobEmbedded/STM32-Tutorials/tree/master/Tutorial%2024-%20NRF24L01%20Radio%20Transceiver>

Appendix A

Microcontroller Circuit

A.1 Pin Out Table

Table A.1: Pin out table

Port	Pin	Function
PA	0	Rotor Pitch 1
PA	1	Rotor Pitch 2
PA	3	SPI 1 Chip Enable
PA	4	SP1 Chip Select 2
PA	5	SPI 1 SCK
PA	6	SPI 1 MISO
PA	7	SPI 1 MOSI
PB	0	Tim3_ch 3 - PWM- Top Motor, Rotor 1
PB	1	Tim3_ch 4 - PWM- Bottom Motor, Rotor 1
PB	3	Green LED for Warning
PB	4	Red LED for warning
PB	5	Tim3_ch 2 - PWM- Bottom Motor, Rotor 2
PC	1	Position Hall Effect Sensor
PC	2	Revolution Hall Effect Sensor
PC	6	Tim3_ch 1 - PWM Top Motor, Rotor 2
PE	1	Red LED for warning

A.2 Full Circuit Diagram

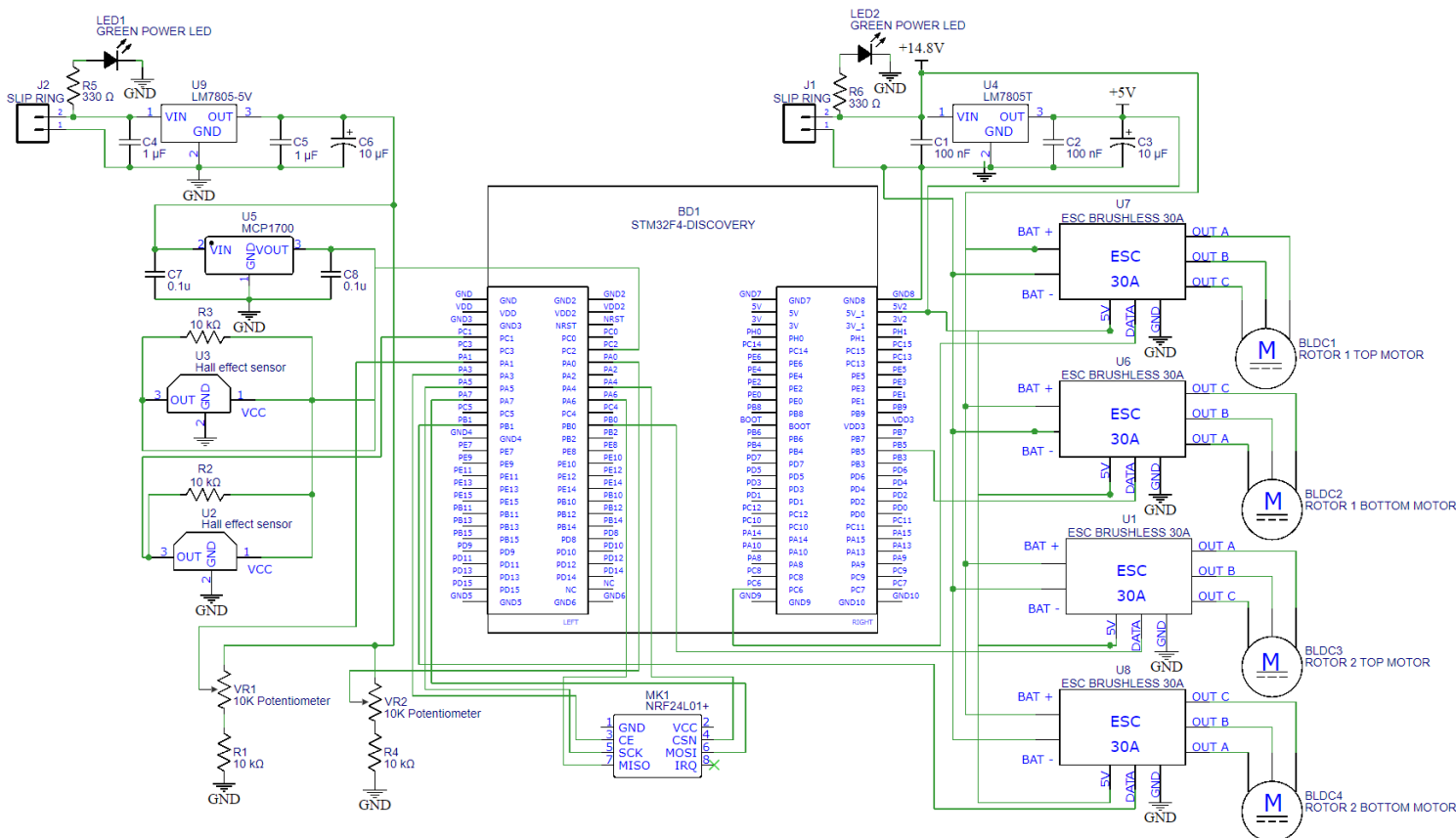
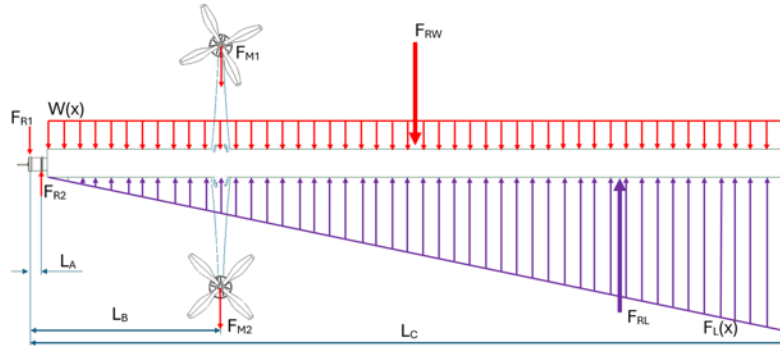


Figure A.1: Circuit Diagram

Appendix B

Mechanical Drawings and Design

Rotor Force Calculations



The length of L_A needs to be found to ensure the 3D printed hub can withstand the force
Variables

$$\begin{aligned}
 m &:= 0.54 \text{ kg} & \text{Weight of the rotor } L_c &:= 0.6 \text{ m} & L_A &:= 0.04 \text{ m} & m_{\text{motor}} &:= 7.5 \text{ g} \\
 g &:= 9.8 \frac{\text{m}}{\text{s}^2} & L_B &:= 0.325 \cdot L_c = 0.195 \text{ m} & L_{AR} &:= L_A + 0.01 \text{ m} = 0.05 \text{ m} & 1 \text{ cm between } F_{R2} \text{ and Rotor} \\
 W &:= \frac{m \cdot g}{L_c} = 8.82 \text{ m Pa} & ABS_{\text{ultimate}} &:= 22.1 \text{ MPa} & (\text{MatWeb,2024})
 \end{aligned}$$

Assume the 3D print is hollow and the only force is from the 2 mm wall at a width of 20 mm
 $\text{wallThickness} := 2 \text{ mm}$ $\text{width} := 20 \text{ mm}$

$$F_{m1} := m_{\text{motor}} \cdot g = 0.0735 \text{ N} \quad F_{m2} := F_{m1}$$

$$F_{RL} := (-20) \text{ N} \quad \text{Maximum expected Thrust}$$

$$F_{RW} := W \cdot L_c + F_{RL} + m_{\text{motor}} \cdot g = -14.6345 \text{ N}$$

$$F_R := F_{RL} \cdot \frac{2 \cdot L_c}{3} + W \cdot L_c \cdot \frac{L_c}{2} + 2 \cdot F_{m1} \cdot L_B = -6.3837 \text{ J}$$

$$F_{R1} := \frac{(L_{AR} - L_A) \cdot F_{RL} + M_R}{L_A} = -164.5934 \text{ N}$$

$$F_{R2} := \frac{(L_{AR}) \cdot F_{RL} + M_R}{L_A} = -184.5934 \text{ N}$$

$$\sigma := \frac{F_{R2}}{\text{wallThickness} \cdot \text{width}} = -4.6148 \cdot 10^6 \text{ Pa}$$

$$\text{SafetyFactor}_{3D\text{Print}} := \left| \frac{ABS_{\text{ultimate}}}{\sigma} \right| = 4.7889$$

Circlip

$$\omega_{max} := 200 \text{ rpm}$$

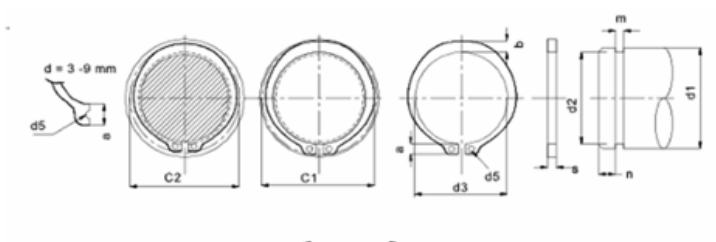
$$F_{normal} := \frac{(\omega_{max} \cdot L_c)^2 \cdot m}{L_c} = ■$$

$$F_{max_Circlip} := 0.4 \text{ kN}$$

$$\text{SafteyFactor}_{\text{circlip}} := \frac{F_{max_Circlip}}{F_{radial}} = 2.8145$$

Circlips - External

Circlips generally to dimensions according to DIN 471

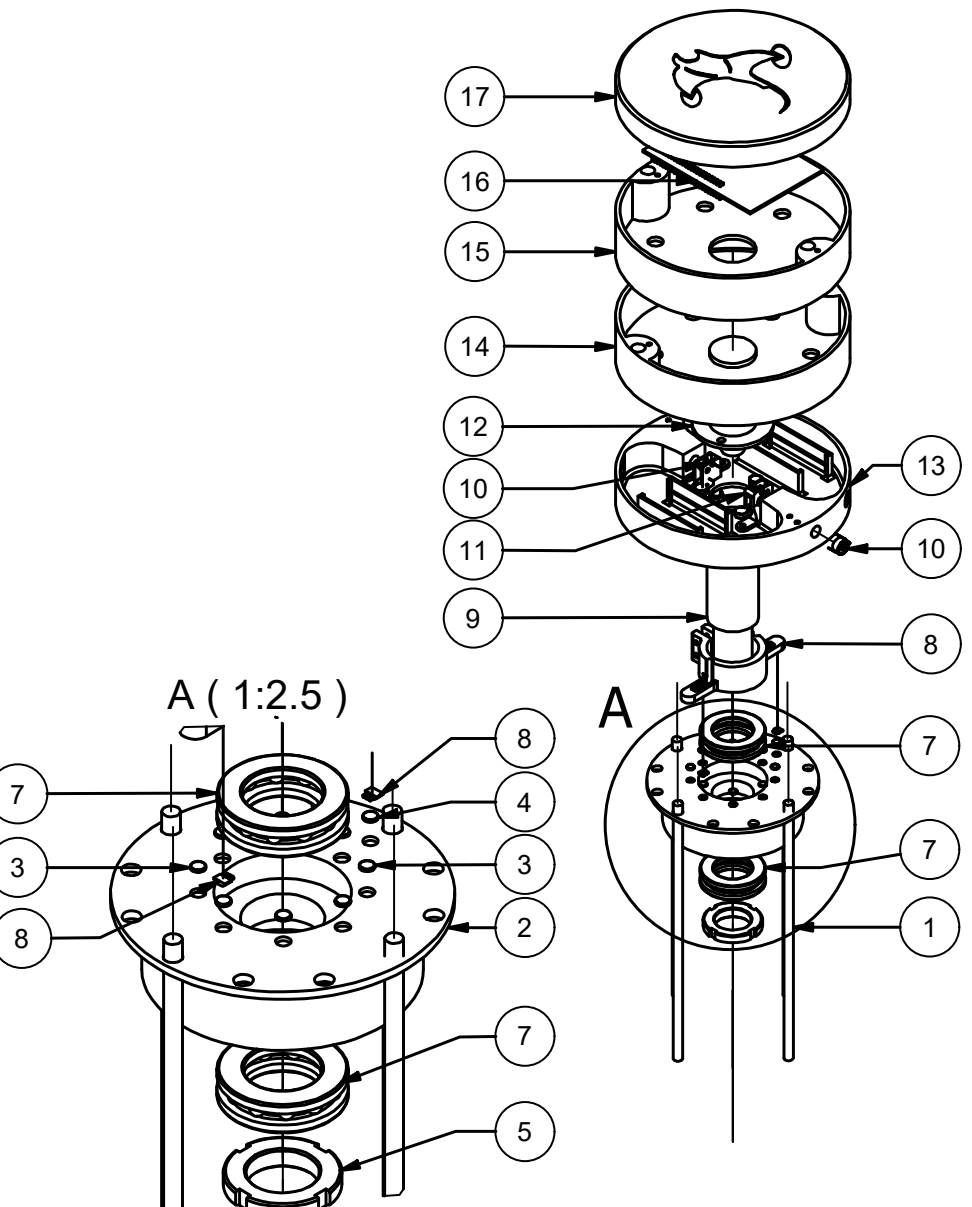


Nom size (mm)	Circlip Dimensions (mm)										Groove Dimensions (mm)				Groove Strength	Circlip Strength
	d ₁	s	s (tol)	d ₃	d ₃ (tol)	a max	b	d smin	C1	C2	d ₂	d ₂ (tol)	m min	t	n	
3	0,40	-0,05	2,7	+0,04 -0,15	1,9	0,8	1,0	7,0	6,6	2,8	-0,04	0,50	0,10	0,3	0,1	0,47
4	0,40	-0,05	3,7	+0,04 -0,15	2,2	0,9	1,0	8,6	8,2	3,8	-0,04	0,50	0,10	0,3	0,2	0,50
5	0,60	-0,05	4,7	+0,04 -0,15	2,5	1,1	1,0	10,3	9,8	4,8	-0,04	0,70	0,10	0,3	0,2	1,0
6	0,70	-0,05	5,6	+0,04 -0,15	2,7	1,3	1,2	11,7	11,1	5,7	-0,04	0,80	0,15	0,5	0,4	1,45
7	0,80	-0,05	6,5	+0,06 -0,18	3,1	1,4	1,2	13,5	12,9	6,7	-0,06	0,90	0,15	0,5	0,5	2,6

6 | 5 | 4 | 3 | 2 | 1

D

D



Parts List

ITEM	DESCRIPTION	Qty.	MATERIAL / SPECIFICATIONS
17	HUB COVER	1	ABS
16	MICROCONTROLLER	1	STM32F407VG DISCOVERY
15	MICROCONTROLLER HUB	1	ABS
14	ELECTRONICS HUB	1	ABS
13	INTERFACE HUB	1	ABS
12	POWER SLIP RING	1	MW 1430
11	POTENTIOMETER MOUNT	2	PLA
10	POTENTIOMETER	2	PT-10 10 kΩ
9	SUPPORT SHAFT	1	BRIGHT STEEL
8	HALL EFFECT SENSOR MOUNT	1	ABS
7	THRUST BALL BEARING	2	55105
6	HALL EFFECT SENSOR	2	AH49E
5	LOCK NUT	1	25×38×7MM M2×X1.5 THREAD
4	ANGULAR VELOCITY MAGNET	1	Ø5 × 2 NEODYMIUM MAGNETS
3	POSITION MAGNETS	8	Ø5 × 2 NEODYMIUM MAGNETS
2	MAIN BODY	1	ABS
1	THREADED RODS	4	M6 STAINLESS STEEL

SCALE ON A4 1:5	TITLE: EXPLODED HUB VIEW		
UNITS IN mm			
STUDENT Nr. 24723061	DRAWN BY RAYDE KRÜGER	CHECKED	DATE
			SHEET Nr. 1 OF 1 SHEETS Nr.061/01/01

STELLENBOSCH UNIVERSITY

STUDENT Nr. 24723061

DRAWN BY RAYDE KRÜGER

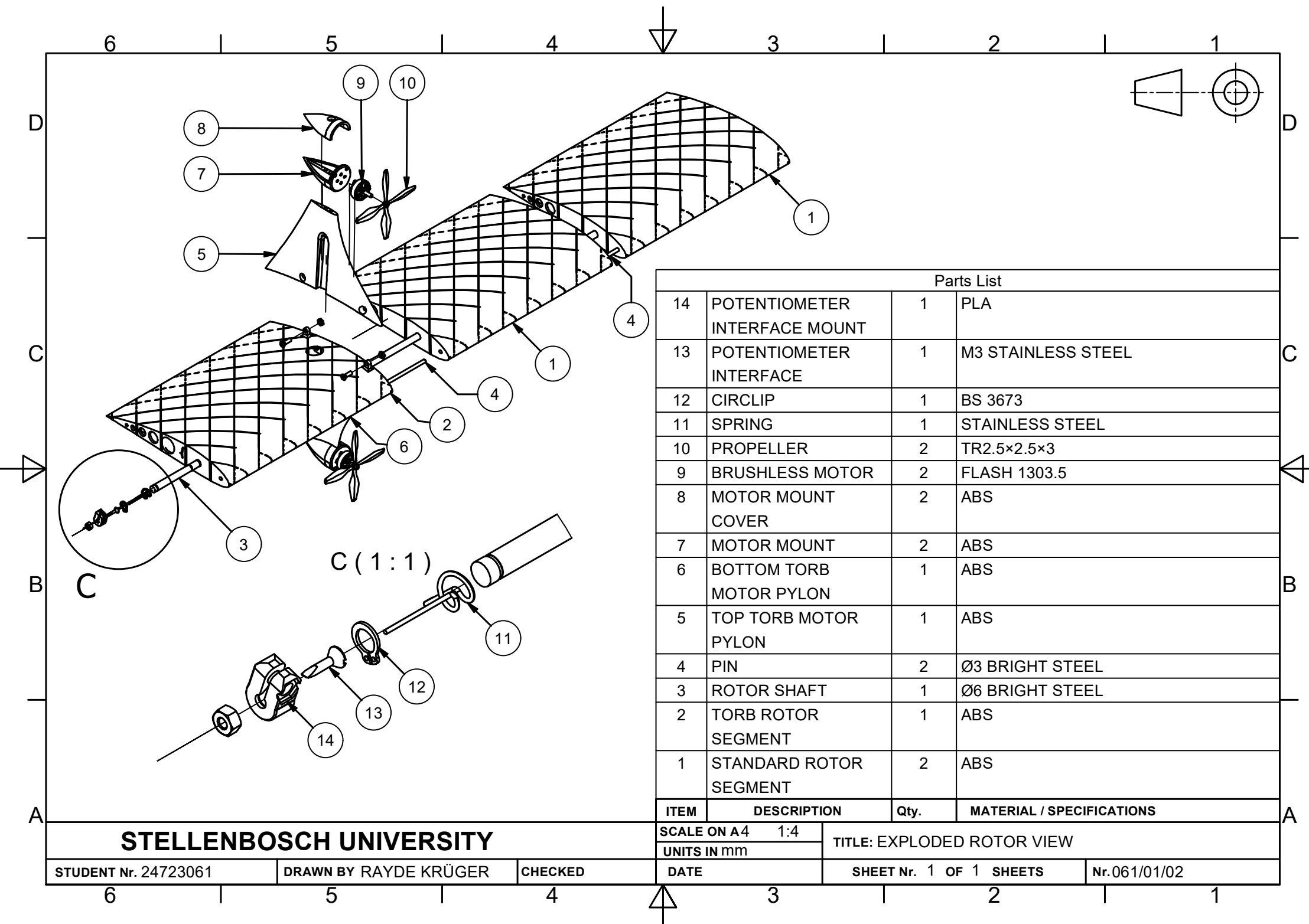
CHECKED

DATE

SHEET Nr. 1 OF 1 SHEETS

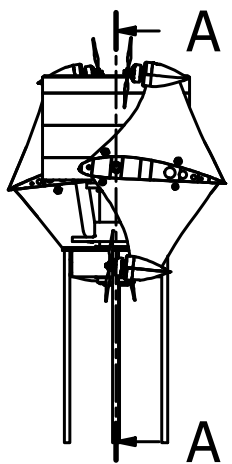
Nr.061/01/01

6 | 5 | 4 | 3 | 2 | 1

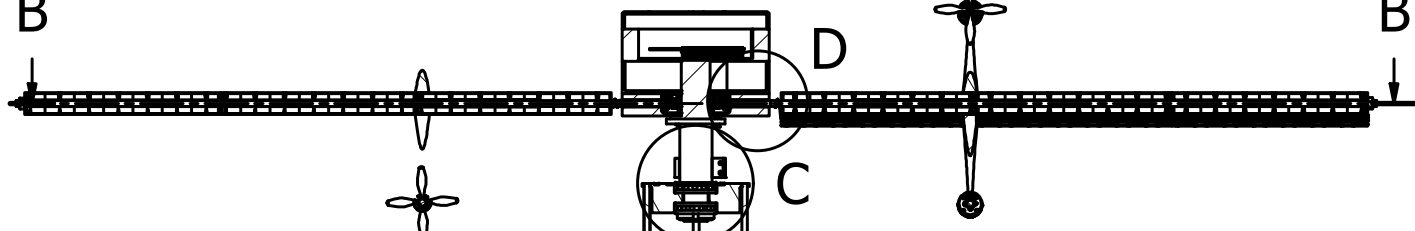


6 | 5 | 4 | 3 | 2 | 1

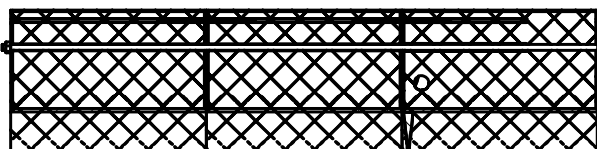
A-A (1 : 8)



B



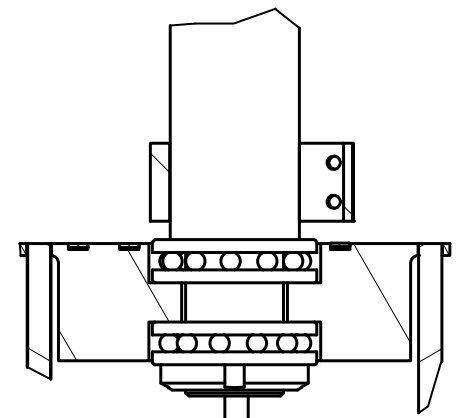
B-B (1 : 8)



2

1

2



C (1 : 2)

DETAILED VIEW OF MAIN BODY
INTERFACE

D (1 : 2)

DETAILED VIEW OF ROTOR
INTERFACE

Parts List			
ITEM	DESCRIPTION	Qty.	MATERIAL / SPECIFICATIONS
2	ROTOR ASSEMBLY	2	061/01/02
1	HUB ASSEMBLY	1	061/01/01
SCALE ON A4 1:5		TITLE: FULL ASSEMBLY DRAWING	
UNITS IN mm			
DATE		SHEET Nr. 1 OF 1 SHEETS	Nr.061/01

STELLENBOSCH UNIVERSITY

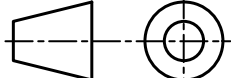
STUDENT Nr. 24723061

DRAWN BY RAYDE KRÜGER

CHECKED

6 | 5 | 4 | 3 | 2 | 1

A-A (1 : 8)



B



C



B



D



C



B



D